Fish Physiol Biochem
DOI 10.1007/s10695-011-9582-0

Impact of silicon-based quantum dots on the antioxidative system in white muscle of *Carassius auratus gibelio*

Loredana Stanca · Sorina Nicoleta Petrache · Mihaela Radu · Andreea Iren Serban · Maria Cristina Munteanu · Daniela Teodorescu · Andreea Cristina Staicu · Cornelia Sima · Marieta Costache · Constantin Grigoriu · Otilia Zarnescu · Anca Dinischiotu

Received: 20 July 2011 / Accepted: 22 November 2011

Abstract Silicon-based quantum dots were intraperitoneally injected in individuals of *Carassius auratus gibelio*. Their effects on white muscle were investigated by following their distribution and impact on the antioxidative system. The GSH level significantly increased after 1 and 3 days of exposure by, respectively, 85.3 and 25.4%. Seven days later, GSH levels were similar to control concentrations. MDA concentration rose after three days by 46.9% and remained at the same level after 7 days. Protein thiol levels significantly decreased by 6.7 and 8.1% after 3 and 7 days, whereas advanced oxidation protein products increased by 12.7, respectively, 28.1% in the same time intervals. The protein reactive carbonyl groups were raised only after the first day of exposure and returned to the control level later on. SOD specific activity increased up to 48% after 7 days, while CAT activity increased by 328, 176, and 26% after 1, 3, and 7 days of treatment. GST specific activity was up-regulated by 87, 18, and 9%, while GR activity increased by 68, 34, and 9%. G6PD activity was up-regulated by 12, 22, and 50%, whereas GPx activity raised by 75 and 109% compared to control after, respectively, 1, 3, and 7 days. Our results suggest that oxidative stress induced by silicon-based quantum dots was not strong enough to cause permanent damage in the white muscle of crucian carp.

Keywords Fish white muscle · Silicon-based quantum dots · Malondialdehyde · Reduced glutathione · Antioxidative enzymes · Protein oxidation

L. Stanca · S. N. Petrache · M. Radu · A. I. Serban · M. C. Munteanu · D. Teodorescu · A. C. Staicu · M. Costache · O. Zarnescu · A. Dinischiotu (✉)
Department of Biochemistry and Molecular Biology, Faculty of Biology, University of Bucharest, 91-95 Splaiul Independetei, 050095 Bucharest, Romania
e-mail: dinischiotu@yahoo.com

A. I. Serban
Department of Preclinical Sciences, Faculty of Veterinary Medicine, University of Agricultural Sciences and Veterinary Medicine, 105 Splaiul Independetei, 050097 Bucharest, Romania

C. Sima · C. Grigoriu
Laser Department, National Institute of Laser, Plasma and Radiation Physics, 409 Atomistilor, 077125 Bucharest-Magurele, Romania

Introduction

Image analysis of biomolecules is a fundamental subject of basic and applied biological and medical research, which can be used in the diagnosis, treatment, and monitoring of several types of chronic diseases (Moghimi et al. 2005). Molecular imaging encompasses various techniques such as magnetic imaging, magnetic resonance spectroscopy, optical bioluminescence, fluorescence imaging, ultrasound, etc., which has the potential to enhance both diagnosis

Published online: 04 December 2011

and management of disease (Bentolila et al. 2009), each of them being characterized by different levels of specificity and sensitivity.

Optical imaging has limitations due to the limited penetration depth of light in living tissue (a few centimeters between 675 and 900 nm) and the insufficient brightness and stability of commonly used organic fluorophores (Bentolila et al. 2009).

Conventional fluorophores are organic substances composed of either chemically synthesized fluorescent dyes or genetically encoded fluorescent proteins. These have several limitations such as short fluorescence duration, narrow excitation, and broad bandwidth emission (Lee 2007).

Nanotechnology improved several imaging techniques with respect to sensitivity and specificity. At present, a vast array of artificial particulate systems are used as imagistic agents, i.e., colloidal gold, paramagnetic iron oxide crystals, dendrimers, liposomes, nanotubes, nanowires, and quantum dots (Debbage and Jaschke 2008).

Quantum dots have been estimated to be up to 20 times brighter and 100 times more stable than traditional fluorophores (Chan and Nie 1998). They are semiconductor nanocrystals (Micic et al. 1995; Yu and Peng 2002) surrounded by a coating or shell made of a semiconductor material (Chan and Shiao 2008), and they are photostable as well (Pi et al. 2010). They are rather resistant to photobleaching and suitable for multicolor experiments, since nanocrystals with different sizes can be simultaneously excited by a single wavelength of light, resulting in multicolor, symmetrical spectral emission (Bruchez et al. 1998). These nanoparticles can be used as fluorescent probes for biomedical applications especially cellular imaging due to an intense and photostable fluorescence (Zhang and Monteiro- Riviere 2009). It can be tuned to emit in the near IR region of the spectrum, in which tissue auto-fluorescence is considerably reduced and excitation light penetration increased. They have been used for tumor targeting and imaging (Gao et al. 2004; Zhang et al. 2008; Sun et al. 2010) as well as vascular mapping and cellular trafficking (Walling et al. 2009). They can be targeted toward specific cells by conjugating them with ligands or antibodies.

Additionally, they can be non-specifically introduced into cells, and thus are able to serve as a potential tracking marker for cellular imaging. Several imaging studies have been done in vitro, using cell cultures (Jamieson et al. 2007; Muller-Borer et al. 2007; Mahto et al. 2010).

Many biological processes cannot be reproduced in cultured cells and often the three-dimensional environment of cells determines their function (Chakraborty et al. 2009). In cultured cells systems, physiological conditions and complex interactions among different cell types and tissues are lacking. Moreover, cell lines are usually transformed and present some traits that are different compared to those of cells in living organisms. In vivo studies are mandatory because exposure to a xenobiotic, which could be an imagistic agent, involves its metabolism by different pathways, excretion and interrelations among different tissues. Usually, in vivo assays are performed after the in vitro ones.

In the past few years, fish have become alternative models among non-mammalian species for toxicity studies, helping to elucidate mechanisms of human diseases such as cancer (Raisuddin and Lee 2008; Mitchell et al. 2010) and aging (Gerhard 2007). The use of mammalian models (mouse, rat) in medical and pharmaceutical research is hampered by high costs. Fish species present the ability to reproduce successfully in a fluctuating environment and to grow rapidly to harvestable sizes (Moyle and Cech 2004).

Recently, zebrafish (*Danio rerio*) was used for imaging experiments (Rieger et al. 2005; Son et al. 2009).

Different fish genera and/or genetic hybrids from interspecific crosses have been used for human health research. Such examples include *Oryzias* (Wittbrodt et al. 2002), *Xiphophorus* (Mitchell et al. 2010), *Pimephales*, *Oncorhynchus*, *Kryptolebias* (Raisuddin and Lee 2008), *Astyanax* (Albertson et al. 2009), and *Danio* (Lieschke and Currie 2007).

Several investigators have proven that quantum dots generate reactive oxygen species in in vivo and in vitro treatments (Bakalova et al. 2004; Green and Howman 2005; Lovric et al. 2005; Chan and Shiao 2008).

There are few studies on the biological applications of silicon quantum dots compared to their heavy metal counterparts, even though they are largely produced by a variety of routes (O'Farrell et al. 2006), and these were focused on the motility assay of heavy meromyosine and actin from the skeletal muscle of the rabbit (Månsson et al. 2004) and the labeling and

tracking of the mesenchymal stem cells (Muller-Borer et al. 2007).

Taking into account that the toxicity of silicon-based quantum dots was less studied, the aim of our paper was to study the effects of these nanoparticles on the redox status of the white muscle of *Carassius auratus gibelio*. The distribution of quantum dots was highlighted by fluorescent image analysis. A set of characteristic parameters was analyzed, such as the activities of superoxide dismutase (SOD) and catalase (Catala 2010), as well as the glutathione antioxidant system, consisting of reduced glutathione (GSH) content and glutathione reductase (GR), glutathione peroxidase (GPx), and glutathione S-transferase (GST) activities. Oxidative stress markers (lipid peroxidation, carbonyl derivatives, thiol proteins, and advanced oxidation protein products) were also determined.

Materials and methods

Chemicals

Nicotinamide adenine dinucleotide phosphate disodium salt ($NADP^+$), nicotinamide adenine dinucleotide phosphate reduced tetrasodium salt (NADPH), and malondialdehyde tetramethyl acetal were supplied by Merck (Darmstadt, Germany), whereas 2,4- dinitrophenylhydrazine was supplied by Loba-Chemie. All the other chemicals used were of analytical grade and were supplied by Sigma (St. Louis, USA).

Nanoparticles

The SiO_2/Si nanoparticles were prepared by pulsed laser ablation technique (Grigoriu et al. 2004). The particles are spherical with a crystalline Si core covered with an amorphous SiO_2 layer (1–1.5-nm thick). The size distribution estimated from transmission electron microscopy image statistics was a lognormal function, in the range of 2–10 nm, with the arithmetic mean value of the diameter of about 5 nm. The nanoparticles excited with a wavelength of 325 nm exhibited a strong red luminescence, clearly visible to the naked eye in daylight. The photoluminescence emission (Grigoriu et al. 2005) consisted of a broadband spectrum in the approximate range of 400 to more than 800 nm.

For the experiments, a suspension of nanoparticles (2 mg/mL) in 7‰ NaCl solution was prepared.

Fish maintenance and treatments

The freshwater crucian carp *Carassius auratus gibelio* with a weight of 90 ± 10 g and a standard length of 13 ± 2 cm, respectively, were acquired from The Nucet Fishery Research Station, Romania. The fish were acclimated to laboratory conditions for 3 weeks prior to the experiment. Water quality characteristics were determined. The mean values for tested water qualities were as follows: temperature 19 ± 2°C, pH (7.4 ± 0.05), dissolved oxygen 6 ± 0.2 mg/L (constant aeration), and total hardness as $CaCO_3$ 175 mg/L. The fish were maintained on a photoperiod with 12 h light/12 h dark. Feeding of pellet food at a rate of 1% of the body weight per day was finished 2 days before initiation of the experiment, and no food was supplied to the fish during the experimental period. During the experiment, no obvious changes in body weight of any fish during the 7 days of experiment were recorded.

Animal maintenance and experimental procedures were in accordance with the *Guide for The Use and Care of Laboratory Animals* (European Communities Council Directive 1986), and efforts were made to minimize animal suffering and to reduce the number of specimens used.

After the acclimatization period, the fish were randomly divided into three groups of 15 individuals each and placed in separate glass aquaria (250 L). Group I was maintained in dechlorinated tap water as a control. Group II was formed by fish intraperitoneally injected with NaCl 7‰ solution, and group III was intraperitoneally injected (IP) with 2 mg quantum dots/kg body weight. After 1, 3, and 7 days, respectively, five fish from each group were cervically dislocated under light ether anesthesia and white muscles were dissected. Tissues were immediately frozen in liquid nitrogen and stored at –80°C until analyses were performed.

Fluorescent image analysis of nanoparticles distribution

Fragments of crucian carp white skeletal muscle were fixed in Bouin solution or 4% paraformaldehyde in PBS, dehydrated in ethanol, cleared in toluene, and

embedded in paraffin. 6 µm-thick sections were used for fluorescence microscopy. After deparaffination and rehydration, slides were stained with 4,6-diamidino-2-phenylindole (DAPI) solution, mounted in PBS, and analyzed by epifluorescence microscopy using a DAPI/FITC/Texas red triple band filter set (Zeiss). Under ultraviolet excitation, silicon-based quantum dots appeared red and nuclei appeared blue with DAPI. The photomicrographs were taken with a digital camera (AxioCam MRc 5, Carl Zeiss) driven by Axio-Vision 4.6 software (Carl Zeiss).

Preparation of tissue homogenates

Homogenates (prepared as 1 g of tissue per 10 volumes of buffer) of fish white muscle were prepared in ice-cold buffer (0.1 M TRIS–HCl, 5 mM EDTA buffer, pH 7.4) using a Potter–Elvehjem homogenizer. A few crystals of the protease inhibitor phenylmethylsulfonyl fluoride were added in the homogenates. The resulting homogenate was centrifuged at 8,000 *g* for 30 min in a Hettich centrifuge at 4°C. The supernatant was decanted and used for analyses.

Biochemical analysis

Glutathione assay

The cellular lysate, deproteinized with 5% sulfosalicylic acid, was analyzed for total glutathione and oxidized glutathione (GSSG) using the Detect X® Glutathione colorimetric detection kit (Arbor Assay USA). Kit supplier instructions were followed in order to determine the total and oxidized glutathione. GSH concentration was obtained by subtracting the GSSG level from the total glutathione. The total and GSH levels were calculated as nmoles/mg protein.

Malondialdehyde assay

The method of del Rio (del Rio et al. 2003) was used to assess malondialdehyde (MDA), as a marker of lipid peroxidation. For 200 µL of sample with a protein concentration of 2 mg/mL, 700 µL 0.1 N HCl was added, and the mixture was incubated for 20 min at room temperature. Then, 900 µL of 0.025 M thiobarbituric acid (TBA) was added, and the total volume was incubated for 65 min at 37°C. Finally, 400 µL of 0.1 M Tris–HCl, 5 mM EDTA buffer, pH 7.4 was added. The fluorescence of MDA was recorded using a 520/549 nm (excitation/emission) filter. A calibration curve with MDA tetramethyl acetal in the range of 0.05–5 µM was used to calculate the MDA concentration. The results were expressed as nmoles of MDA/mg protein.

Protein sulfhydryls assay

The protein sulfhydryl concentration was done according to a slightly adapted version of the Ellman's method (1959), (Riener et al. 2002). A volume of 100 µL of total protein extract was mixed with 100 µL 10% sulfosalicylic acid and vortexed three times. After 10 min on ice, the sample was centrifuged for 10 min at 10,000 rpm at room temperature. The pellet was rendered soluble in 20 µL of 1 M NaOH, and 730 µL of 0.4 M TRIS buffer pH 9 was added. After 5 min at room temperature, 20 µL of 5 mM 5,5-Dithio-bis(2-nitrobenzoic acid) (DTNB) prepared in 100% methanol was supplemented, and the absorbance at 412 nm was measured immediately. The concentration of protein sulfhydryl groups was quantified using N-acetyl-cysteine standard curve.

Advanced oxidation protein products assay

The concentration of advanced oxidation protein products (AOPP) was assessed according to the method of Witko-Sarsat et al. (1992). A sample of 200 µL total protein extract was mixed with 10 µL 1.16 M potassium iodide and vortexed for 5 min at room temperature. A volume of 20 µL of glacial acetic acid was added, and the mixture was vortexed again for 30 s. The optical density of samples was read at a wave length of 340 nm in a 96-well plate using a Tecan Genios Multireader. The AOPP level of samples was calculated using a chloramines-*T* standard curve (100 µM stock solution).

Reactive carbonyl groups in proteins

The reactive carbonyl groups in proteins (RCGP) were measured according to the method of Fields and Dixon (1971). A volume of 500 µL sample diluted accordingly was incubated with 10 mM 2,4-dinitrophenylhydrazyne prepared in 2 M HCl, for 1 h, at room temperature with vortex every 15 min. After incubation, a volume of ice-cold 500 µL 20% TCA

was added, and the mixture was kept on ice for 30 min. The samples were then centrifuged at 13,000 rpm for 3 min at 4°C. The pellets were washed with 1 mL mixture 1:1 ethanol/ ethyl acetate and rested for 10 min at room temperature. Then, the samples were centrifuged again at 13,000 rpm, for 3 min at 4°C. The wash was repeated twice. The pellet was solved in 600 µL of 1 M NaOH, and the absorbance was read at 370 nm, against a blank of 1 M NaOH. The carbonyl levels were calculated using a molar extinction coefficient of 22,000 $M^{-1} \times cm^{-1}$ (Fields and Dixon 1971).

Enzyme activity assays

SOD (EC 1.15.1.1) was assayed according to the method of Paoletti and Mocali, based on NADPH oxidation (Paoletti and Mocali 1990). The decrease in absorbance at 340 nm was followed for 10 min to allow NADPH oxidation by the generated superoxide anion. A control was run with each set of three duplicate samples, and the percent inhibition was calculated as (sample rate)/(control rate) × 100. One U of SOD activity was defined as half-maximal inhibition.

CAT (EC 1.11.1.6) activity was assayed by monitoring the disappearance of H_2O_2 at 240 nm (Aebi 1974). CAT specific activity was calculated in terms of U/mg protein, where 1U is the amount of enzyme that catalyzed the conversion of 1 µmol H_2O_2 in a minute.

G6PDH (EC 1.1.1.49) glucose 6-phosphate dehydrogenase activity was measured according to Lohr's method. The rate of the NADPH formation was a measure of G6PDH activity, and this can be followed by means of the increase in extinction at 340 nm (Lohr and Waller 1974).

Total GPx (EC 1.11.1.9) activity was assayed by Beutler's method, using tert-butyl hydroperoxide and GSH as substrates (Beutler 1984). The conversion of NADPH to $NADP^+$ due to the reduction of GSSG to GSH by GR was followed by recording the changes in absorption intensity at 340 nm. One unit was expressed as 1 µmol of NADPH consumed per minute, using a molar extinction coefficient of 6.22×10^3 M^{-1} cm^{-1}.

GST (EC 2.5.1.18) activity was assayed spectrophotometrically at 340 nm by measuring the rate of chloro-dinitrobenzene (CDNB) conjugation with GSH (Habig et al. 1974). One unit of GST activity was defined as the formation of 1 µmol of conjugated product per minute. The extinction coefficient 9.6 $mM^{-1}cm^{-1}$ of CDNB was used for the calculation.

GR (EC 1.6.4.2) activity was determined according to Golberg and Spooner's method, in 0.1 M phosphate buffer, pH 7.4 with 0.66 mM GSSG and 0.1 mM NADPH. One unit of GR activity was calculated as 1 µmol of NADPH consumed per minute (Goldberg and Spooner 1983).

Protein concentration assay

The protein content was determined using Lowry's method with bovine serum albumin as standard (Lowry et al. 1951). All the enzymatic activities, calculated as specific activities (units/mg of protein), were expressed as % from controls.

Statistical analysis

All values were expressed as means ± SE. The differences between control and quantum dots-treated experimental group were analyzed by Student's *t* test and validated by confidence intervals using Quattro Pro X3 software. The results were considered significant only if the *P* value was less than 0.05, and confidence intervals of control and samples did not overlap.

Results

Microscopical studies

Due to intrinsic photoluminescence under ultraviolet excitation, silicon-based quantum dots have been detected in tissue sections by the emission of red light (Fig. 1b–f). The fluorescence was not detectable for the control (non-injected and injected with NaCl 7‰) animals (Fig. 1a). Histological examination of the white skeletal muscle has indicated that silicon-based quantum dots accumulated in the sarcoplasm at all time intervals (1, 3 and 7 days), with the most intense accumulation being detected at 7 days after IP injections (Fig. 1e, f). The uptake of silicon-based quantum dots varied among white skeletal muscle fibers. From this point of view, at the same time intervals, white skeletal muscle from each fish showed heterogeneous staining patterns with discrete staining of some muscle fibers (Fig. 1c), whereas

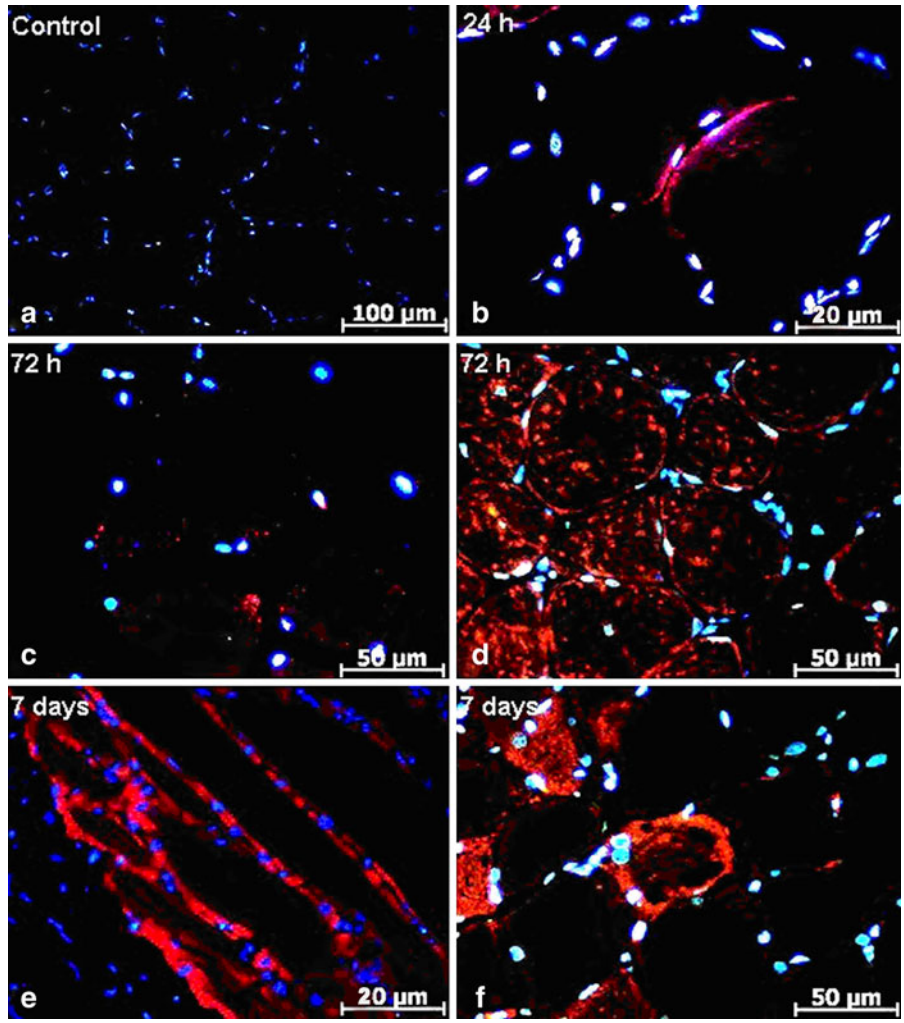

Fig. 1 Silicon-based quantum dots localization in the white skeletal muscle of *Carassius auratus gibelio*. **a** Control (non-injected) animals. **b** Visualization of silicon-based quantum dots transfer to white skeletal muscle at 24 h after IP injection. Discrete (**c**) and intense (**d**) staining pattern of muscle fibers at 72 h after IP injection. At 7 days after IP injection, silicon-based quantum dots accumulate in subsarcolemmal space (**e**) and inside of some muscle fibers (**f**). Muscle fibers loaded with silicon-based quantum showed degenerative changes like vacuolization (**f**) at 7 days after IP injection

others were intensely stained (Fig. 1d), probably due to their location in the vicinity of blood vessels. Muscle fibers seemed to accumulate nanoparticles in the subsarcolemmal space and inside the muscle fibers (Fig. 1e). At 7 days after IP injection, some muscle fibers loaded with silicon-based quantum dots showed degenerative changes like vacuolization (Fig. 1f).

Lipid peroxidation

MDA concentration (Table 1) did not change after the first day, but significantly increased by 46.9% after 3 days compared to control. After 7 days, its level remained unchanged compared to samples of the 3 day exposure.

GSH level

A significant increase of the GSH level was observed in the white muscle of fish intraperitoneally injected with silicon-based quantum dots after 1 day exposure, being almost double compared to the control. After 3 days, the GSH concentration decreased by about 67.5% compared to the day one samples, but it was

Table 1 The relative values of malondialdehyde and reduced glutathione, in the white muscle of *Carassius auratus gibelio* IP injected with silicon-based quantum dots (2 mg/kg body weight)

Time (days)	MDA (nmoles/mg)	GSH (nmoles/mg)
Control	100 ± 12.3	100 ± 9.3
1	105.1 ± 13.4	185.3 ± 14*
3	146.9 ± 17.3***	125.4 ± 1.9*
7	144.2 ± 15.3***	97.4 ± 4.9

Data are calculated as means ± SD ($n = 5$ in each group at each time point) and expressed as % from time point controls; * $P < 0.05$, *** $P < 0.001$

about 25.4% higher compared to control values. By the seventh day, the GSH level reached the control value (Table 1).

Oxidative alterations at protein level

The protein thiol level decreased significantly by 6.7 and 8.1% after 3 and 7 days of treatment, respectively, compared to control. Also, AOPP concentration significantly increased by 12.7 and 28% after 3 and 7 days of treatment compared to control, whereas PRCG level significantly increased only after the first day of exposure and later on returned to the control level (Table 2).

The antioxidant scavenging enzymes

Figure 2 shows the effects of silicon-based quantum dots exposure on the activities of antioxidant enzymes SOD and CAT, in the white muscle of *C. auratus gibelio*. A slight decrease of SOD specific activity was noticed after 1 day of exposure, whereas after 3 and 7 days it increased by 33 and 48%, respectively. CAT activity increased by 328, 176, and 26% after 1, 3, and 7 days of treatment.

Enzymes involved in GSH metabolism

The variation in the specific activities of the enzymes involved in GSH metabolism, i.e., GPx, GR, and GST are presented in Fig. 3. GPx activity was down-regulated by 6% after 1 day of treatment. For the other time points, it increased by 75 and 109%.

After 1 day of treatment, the level of GR specific activity increased by 68% in comparison with control, whereas after 3 days exposure, this activity was diminished by 35% compared to the former level, but still 34% higher compared to control. After 7 days, GR activity decreased by 9% compared to control.

Significant up-regulation of GST specific activity by 87, 18, and 9% compared to controls was recorded after 1, 3, and 7 days of exposure, respectively.

Enzyme generating reducing equivalents

G6PD plays a key role in the maintenance of cellular redox potential via production of NADPH (Kletzien et al. 1994). In our experiment, its specific activity was up-regulated by 12, 22, and 50% after 1, 3, and 7 days of fish exposure to QDs (Fig. 4).

Discussion

The silicon-based QDs used in this study were produced to emit in the NIR region of the spectrum, in which the autofluorescence of tissues is significantly reduced and excitation light penetration increased (Grigoriu et al. 2005). QDs are photostable and suitable for long-term observation or repeated measurements (Bentolila et al. 2009).

In our experiment, individuals of *Carassius auratus gibelio* were used due to the fact that they are widely spread in freshwaters. They are also common in

Table 2 The relative values of proteic thiols and advanced oxidation protein products (AOPP) and protein reactive carbonyl groups (PRCG) in the white muscle of *Carassius auratus gibelio* IP injected with silicon-based quantum dots (2 mg/kg body weight)

Time (days)	Proteic thiols (nmoles/mg)	AOPP (nmoles/mg)	PRCG (nmoles/mg)
Control	100 ± 2	100 ± 8.2	100 ± 9.4
1	97.3 ± 3.8	98.7 ± 14.9	114.2 ± 14.4*
3	93.3 ± 4.5*	112.7 ± 11.3**	106.7 ± 15.9
7	91.9 ± 4.6*	128.1 ± 8.6***	99.6 ± 11.2

Data are calculated as means ± SD ($n = 5$ in each group at each time point) and expressed as % from time point controls); * $P < 0.05$, ** $P < 0.01$, *** $P < 0.001$

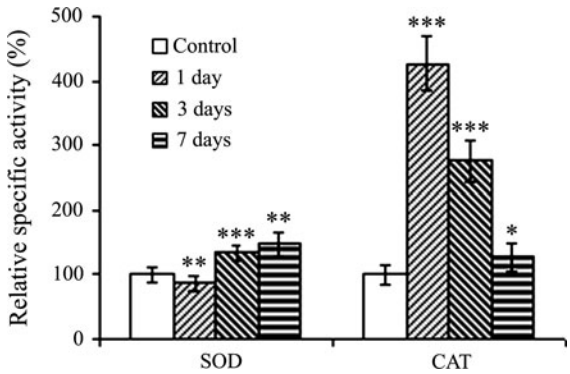

Fig. 2 SOD and CAT specific activities in the white muscle of *Carassius auratus gibelio* IP injected with silicon-based quantum dots (2 mg/kg body weight) up to 7 days of exposure. Activities are calculated as means ± SD ($n = 5$ in each group at each time point) and expressed as % from controls. $^{*}P < 0.05$, $^{**}P < 0.01$, $^{***}P < 0.001$

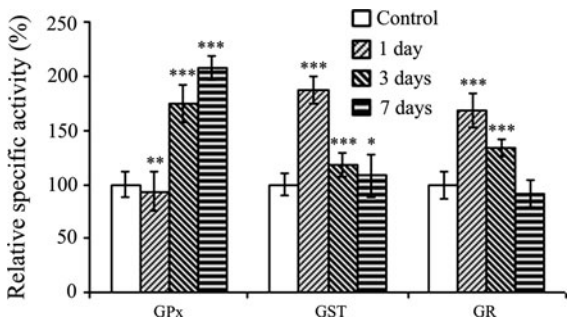

Fig. 3 GPX, GST, and GR specific activities in the white muscle of *Carassius auratus gibelio* IP injected with silicon-based quantum dots (2 mg/kg body weight) up to 7days of exposure. Activities are calculated as means ± SD ($n = 5$ in each group at each time point) and expressed as % from controls. $^{*}P < 0.05$, $^{**}P < 0.01$, $^{***}P < 0.001$

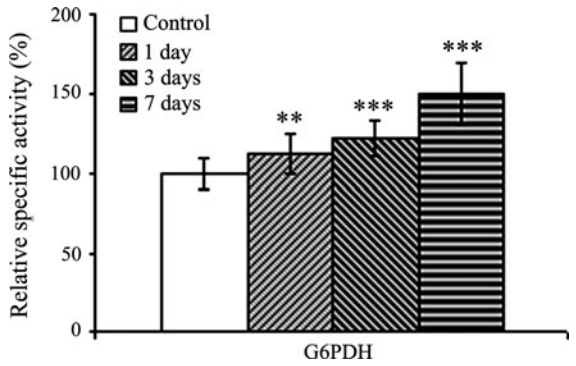

Fig. 4 Variation of G6PD specific activity in the white muscle of *Carassius auratus gibelio* IP injected with silicon-based quantum dots (2 mg/kg body weight) up to 7 days of exposure. Activities are calculated as means ± SD ($n = 5$ in each group at each time point) and expressed as % from controls. $^{*}P < 0.05$, $^{**}P < 0.01$, $^{***}P < 0.001$

aquaculture and quite tolerant to xenobiotic exposure (De Boeck et al. 2003; Dinu et al. 2010), temperature (Ford and Beitinger 2005), dissolved oxygen, pH changes (Olaviyan 1975), etc.

The QDs injected intraperitoneally were taken up by blood circulation and spread to all organs, especially in fish white muscle as well as in liver, red muscle, and kidney (data not shown). Once accumulated in tissues, QDs enter the cells by endocytosis (Chang et al. 2006; Li et al. 2009).

To date, few studies about toxicity of nanoparticles have been done on fish (Federici et al. 2007; Zhu et al. 2010; Shaw and Handy 2011). So far, most of the work on tissue distribution of nanoparticles has been restricted to rodents (Kim et al. 2006; Gatti et al. 2008; Cho et al. 2009; Park et al. 2009; Xie et al. 2010; Liu et al. 2011). The present study, as far as we know, is the first report describing silicon-based quantum dots distribution in fish white muscle. Previous studies on mice have indicated that silica nanoparticles mostly accumulate in the organs of the reticuloendothelial system, such as liver and spleen, and also in the kidney (Cho et al. 2009; Xie et al. 2010; Liu et al. 2011). Studies performed on rat skeletal muscle have shown that endocytosis occurs over the entire muscle fiber, and fluid phase markers were transported into perinuclear and interfibrillar structures (Kaisto et al. 1999). These findings are in accordance with the results from the present study showing that silicon-based quantum dots accumulate in subsarcolemmal space (perinuclear) and inside of white muscle fibers (Fig. 1). In light of the findings in our study, we can, therefore, reasonably speculate that silica nanoparticles were taken up in the white muscle through endocytosis.

Once they entered the myofibers, silicon core nanoparticles covered by silica induced oxidative stress as ascertained by the time-dependent variation of antioxidant enzymes. It seemed that white muscle fibers promoted ROS production (Anderson and Neufer 2006), probably due to NADPH oxidases located within the sarcoplasmic reticulum, transverse tubules, and sarcolemma (Powers and Jackson 2008). The superoxide anion is the result not only of these enzymatic activities but also of cytoplasmic xanthine oxidase (Gomez-Cabrera et al. 2005). The dismutation

of superoxide produces hydrogen peroxide, and this reaction can occur under the catalytical control of superoxide dismutases or spontaneously.

The intracellular production of ROS could play an important role in disturbance of calcium homeostasis, generating calcium overload in cells (Powers et al. 2010), and as a result, Ca^{2+}/calmodulin-dependent enzymes may be activated, resulting in production of nitric oxide and peroxynitrite, a strong oxidizing agent (Moylen and Reid 2007).

In case of our experiment, SOD and CAT activities were shown to be increased in the muscle of QDs exposed fish. It seemed that superoxide generated by silicon-based QDs was dismutated in hydrogen peroxide in the first day after the intraperitoneal injection without SOD catalytic intervention. Due to this fact, CAT specific activity increased tremendously, whereas the SOD one slightly decreased (Fig. 2). Starting with the third day until the seventh day of exposure, SOD probably began to be active and involved in the dismutation reaction, and as a result, its specific activity increased. Although CAT activity decreased, it still remained higher compared to control values. A comparison of Figs. 2 and 3 reveals that the profiles of the specific activity variation of CAT and GPx are inversely proportional, probably because after 1 day of exposure, the generation of hydrogen peroxide was very high and catalase diminished it, thus explaining the reduced level of MDA. After 3 and 7 days of exposure, ROS generation resulted in lipid peroxidation (Table 1), and these products were removed in the reaction catalyzed by GPx. The increased level of MDA after 3 days was maintained after 7 days of exposure as well, suggesting the lipid peroxidation process reached a plateau, which would probably be followed by a decrease after a longer period of exposure, due to the high GPx activity.

The time-dependent variation of GST specific activity was opposite to the GPx one. It is well known that some GST isoforms have a selenium-independent GPx activity. In our case, it seemed that GST activity could be involved in the conjugation of eicosanoids, especially prostaglandins and leukotrienes, which are important mediators of inflammation in fish (Rowley 1996). The high quantity of hydrogen peroxide formed in the first day post-exposure could promote the activation of cytosolic phospholipase A2 (Colston et al. 2005), as well as the high cytosolic Ca^{2+} level probably released from the sarcoplasmic reticulum and damaged mitochondria. Its catalytic activity could generate arachidonic acid, which can be metabolized by cyclic and acyclic pathways resulting in the production of prostaglandins, prostacyclins, thromboxans, and leukotrienes. According to Malis and Bonventre, phospholipase A2 can act synergistically with ROS due to the fact that peroxidized membranes become susceptible to the action of this enzyme (Malis and Bonventre 1986). Previous studies proved that in fish muscle, prostaglandin E_2 is the predominant product of reactions catalyzed by cyclooxygenases 1 and 2 (Grosser et al. 2002). The profile of the variation of GST specific activity suggests that probably after 1 day of exposure, the generation of eicosanoids was high and the enzymes conjugated them, lowering their level and possibly diminishing the pro-inflammatory effect of QDs in white muscle.

Under normal physiological conditions, the total amount of cellular GSH keeps a balance between its synthesis and its utilization. Oxidative stress may be induced when the level of ROS overwhelmed the antioxidant capacity of the analyzed tissue.

GSH plays a pivotal role in redox homeostasis, as it is involved in free radical scavenging, detoxification of electrophils, maintenance of thiol-disulfide status of cysteine-containing proteins, and signal transduction (Sen and Packer 1996). It is an electron-carrier substrate for several enzymes involved in the diminution of ROS level and also reacts directly with radicals in non-enzymatic reactions (Winterbourn and Metodieva 1994). GSH is synthesized from precursor amino acids in the cytosol of all cells through the γ-glutamyl cycle. Whereas this peptide is exported by most cells, it is efficiently imported only into those cells which contain the γ–glutamyl transpeptidase on the outer face of their plasmalemmas. Fish white muscle cells present γ-glutamyl transpeptidase activity (Hegazi et al. 2010). In our experiment, the GSH level significantly increased after the first 3 days and returned to the control values after 7 days (Table 1). It seems that the high glutathione level in these cells was maintained by a high import of γ–glutamyl amino acids as well as by the GR contribution, taking into account that the last enzymatic specific activity decreased in the same time-dependent manner as GSH concentration. GR catalyzes the reaction in which the oxidized disulfide form is reduced in the presence of NADPH generated by the pentose monophosphate pathway. It is possible that direct

interaction of hydroxyl radicals with GSH generated an important quantity of oxidized glutathione (G–S–S–G). The oxidized glutathione was also generated in the reaction catalyzed by GPx. In fact, GR helps the recycling of GSH. In contrast, during the generation of glutathione-S-conjugates by GSTs, the level of intracellular GSH is lowered. Taking into account that GSH level remained almost at control level after the 7-day exposure, it seems that GSH biosynthetic capacity of fish white muscle is important.

According to our results, it appeared that NADPH had a pro-oxidant action and was primarily used for superoxide generation in the reactions catalyzed by NADPH oxidases, while it was also important for GSH regeneration. Probably the synthesis of GSH was the most important process for maintaining its level, in comparison with the regeneration in the reaction catalyzed by GR.

ROS escaped from the action of antioxidative system also attacked the proteins. Additionally, MDA as well as other products of lipids oxidation could covalently bind to lysil, histidyl, and cysteinil residues leading to the formation of Schiff bases adducts on proteins (Haberland et al. 1988). Oxidative alterations of proteins can have either mild or severe effects on cellular or systemic metabolism depending on the quantity of modified proteins and the chronicity of the alterations (Shacter 2000).

It is considered that cysteine and methionine are the most prone to oxidative attack. All oxidizing species can induce their modification (Shacter 2000). The chemical modification of protein thiols by ROS generally occurs by the formation of internal or mixed disulfides with GSH. This disulfides formation can be considered as a form of defense against oxidative damage and can play a role in redox signaling (Filipovska and Murphy 2006). Oxidation of cysteine residues results in a number of derivatives, including disulfides, sulfenic, sulfinic, and sulfonic acids. Taking into account GSH abundance in the white muscle, this is an important co-reactant for protein thiol modification. After 7 days, the decrease of proteic thiols was only 8%, which suggests that thiol groups present on proteins are minor antioxidants in the white muscle of *Carassius auratus gibelio*.

AOPP are formed in vivo following the exposure of proteins to hypochlorous acid (product of myeloperoxidase activity) by deamination of lysyl residues and/or oxidation of tyrosyl, histidyl, and cysteinil residues, and have been considered as markers of oxidant-mediated protein damage (Witko-Sarsat et al. 1996). These closely correlate with the levels of dityrosine (Alderman et al. 2002). To our knowledge, AOPPs have not been detected in fish white muscle until now. We have detected a time-dependent increase of their levels, but this was also mild, compared to pathological conditions (Witko-Sarsat et al. 1998). This rise of AOPP could reflect neutrophil and/or monocyte involvement in the oxidative stress (Hazen et al. 1999) induced by exposure of fish white muscle to QDs.

Carbonyl groups in proteins may be generated by ROS-mediated oxidation of side chains of some amino acid residues (especially proline, arginine, lysine, and threonine) or by glycation and reactions with lipid peroxidation products (Bruchez et al. 1998).

In our experiments, it seemed that the generation of protein carbonyl was due to the first two abovementioned reasons and not to the reaction by lipid peroxidation products, as these two biochemical parameters present inverse proportional variation.

Protein oxidation is a part of degenerative processes (Aksenov et al. 2001; Rajesh et al. 2004; Rutkowska et al. 2005; Torres-Ramos et al. 2009), but in our experiment, its level was moderate. It could be assumed that these modified proteins could be degraded by the proteosomal system, avoiding their cross-linking, agglomeration, and installing of possible pathological situations.

The alteration of biochemical parameters studied by us is similar to those recorded in white muscle of fish exposed to other stressors. So, methyl parathion exposure determined a significant increase of SOD, CAT, and GST, in the freshwater fish *Brycon cephalus* (Monteiro et al. 2006). Also, carbamazepine, a pharmaceutical anticonvulsant commonly present in groundwater, determined raised levels of MDA and PRCG (Li et al. 2010).

Conclusions

Taking into account the elevated GSH level, the cessation of lipid peroxidation, and the low level of oxidative alterations of proteins in the white muscle, it appears that this *Carassius auratus gibelio* tissue has the capacity to cope with oxidative stress under silicon-based quantum dots, possibly due to the

adapted response of the antioxidative enzyme during the exposure. On the other hand, the poor blood supply and lack of myoglobin in fish white muscle could be contributing factors to this behavior.

A longer term study would indicate the period of time in which these biochemical parameters would return to control values and, as a consequence, how safe is the use of these QDs in imagistic studies.

Acknowledgments This study was financially supported by the National Research Council of Higher Education, Romania, grant number 127TE/2010 and Grant POSDRU 88/1.5/S/61150/2010 co-financed from European Social Fund by the Sectorial Operational Program for Development of Human Resources 2007–2010. The authors are grateful to COST CM1001/2010 Action for the opportunity to change ideas with experts in post-translational modifications of proteins. We also thank Prof. Radu Burlacu for his advice concerning statistical analysis.

References

Aebi H (1974) Catalase. In: Bergmeyer HU (ed) Methods of enzymatic analysis. Academic Press, New York and London, pp 673–677

Aksenov MY, Aksenova MV, Butterfield DA, Geddes JW WRM (2001) Protein oxidation in the brain in Alzheimer's disease. Neuroscience 103:373–383

Albertson RC, Cresko W, Detrich IHW, Postlethwait JH (2009) Evolutionary mutant models for human disease. Trends Genet 25:74–81

Alderman CJ, Shah S, Foreman JC, Cham BM, Katz DR (2002) The role of advanced oxidation protein products in regulation of dendritic cell function. Free Rad Biol Med 32:377–385

Anderson EJ, Neufer PD (2006) Type II skeletal myofibers possess unique properties. That potentiate mitochondrial H_2O_2 generation. Am J Physiol Cell Physiol 290:844–851

Bakalova R, Ohba H, Zhelev Z, Nagase T, Jose R, Ishikawa M, Baba Y (2004) Quantum dot anti-CD conjugate: are they potential photosensitizers or potentiators of classical photosensitizing agents in photodynamic therapy of cancer? Nano Lett 4:1567–1573

Bentolila LA, Ebenstein Y, Weiss S (2009) Quantum dots for in vivo small-animal imaging. J Nucl Med 50:493–496

Beutler E (1984) Red cell metabolism. In: Beutler E (ed) A manual of biochemical methods. Grune and Stratton, Orlando, pp 68–73

Bruchez M, Moronne M, Gin P, Weiss S, Alivisatos AP (1998) Semiconductor nanocrystals as fluorescent biological labels. Science 281:2013−2016

Catala A (2010) A synopsis of the process of lipid peroxidation since the discovery of the essential fatty acids. Biochem Biophys Res Commun 399:318–323

Chakraborty C, Hsu CS, Wen ZH, Lin CS, Agoramoorthy G (2009) Zebrafish: A complete animal model for in vivo drug discovery and development. Curr Drug Metab 10: 116–124

Chan WCW, Nie S (1998) Quantum dot bioconjugates for ultrasensitive nonisotopic detection. Science 281:2016–2018

Chan W-H, Shiao N-H (2008) Cytotoxic effect of CdSe quantum dots on mouse embryonic development. Acta Pharmacol Sin 28:259–266

Chang E, Thekkek N, Yu WW, Colvin VL, Drezek R (2006) Evaluation of quantum dot toxicity based on intracellular uptake. Small 2:1412–1417

Cho M, Cho WS, Choi M, Kim SJ, Han BS, Kim SH, Kim HO, Sheen YY, Jeong J (2009) The impact of size on tissue distribution and elimination by single intravenous injection of silica nanoparticles. Toxicol Lett 189:177–183

Colston JT, de la Rosa SD, Strader JR, Anderson MA, Freeman GL (2005) H_2O_2 activates Nox4 through PLA2-dependent arachidonic acid production in adult cardiac fibroblast. FEBS Lett 579:2533–2540

De Boeck G, Ngo TTH, Van Campenhout K, Blust R (2003) Differential metallothionein induction patterns in three freshwater fish during sublethal copper exposure. Aquat Toxicol 65:413–424

Debbage P, Jaschke W (2008) Molecular imaging with nanoparticles: giant roles for dwarf actors. Histochem Cell Biol 130:845–875

del Rio D, Pellegrini N, Colombi B, Bianchi M, Serafini M, Torta F, Tegoni SM, Musci M, Brighenti F (2003) Rapid fluorimetric method to detect total plasma malondialdehyde with mild derivatization conditions Clin Chem 49:690–692

Dinu D, Marinescu D, Munteanu MC, Staicu AC, Costache M, Dinischiotu A (2010) Modulatory effects of deltamethrin on antioxidant defence mechanisms and lipid peroxidation in *carassius auratus gibelio* liver and intestine. Arch Env Contam Toxicol 58:757–764

Federici G, Shaw BJ, Handy RD (2007) Toxicity of titanium dioxide nanoparticles to rainbow trout (Oncorhynchus mykiss): Gill injury, oxidative stress and other physiological effects. Aquatic Toxicol 84:415–430

Fields R, Dixon HBF (1971) Micro method for determination of reactive carbonyl groups in proteins and peptides, using 2, 4-dinitrophenylhydrazine. Biochem J 121:587–589

Filipovska A, Murphy MP (2006) Overview of protein glutathionylation. Curr Protocols Toxicol 28:6.10.11–16. 10.18

Ford T, Beitinger TL (2005) Temperature tolerance in the goldfish, *Carassius auratus*. J Therm Biol 30:147–152

Gao X, Cui J, Levenson RM, Chung LW, Nie S (2004) In vivo cancer targeting and imaging with semiconductor quantum dots. Nat Biotechnol 22:969–976

Gatti AM, Kirkpatrick J, Gambarelli A, Capitani F, Hansen T, Eloy R, Clermont G (2008) ESEM evaluations of muscle/nanoparticles interface in a rat model. J Mater Sci Mater Med 19:1515–1522

Gerhard GS (2007) Small laboratory fish as models for aging research. Ageing Res Rev 6:64–72

Goldberg DM, Spooner RJ (1983) Glutathione reductase. In: Bergmeyer HU (ed) Methods of enzymatic analysis, vol 111. Verlag Chemie, Weinheim, pp 258–265

Gomez-Cabrera MC, Borrás C, Pallardó FV, Sastre J, Ji LL, Vinã J (2005) Decreasing xanthine-oxidase -mediated oxidative stress prevents useful cellular adaptation to exercise in rats. JPhysiol 567:113–120

Green M, Howman E (2005) Semiconductor quantum dots and free radical induced DNA nicking. Chem Commun 1: 121–123

Grigoriu C, Nicolae I, Ciupina V, Prodan G, Suematsu H, Yatsui K (2004) Influence of the experimental parameters on silicon nanoparticles produced by laser ablation. J Optoelectr Adv Mat 6:825–830

Grigoriu C, Kuroki Y, Nicolae I, Zhu X, Hirai M, Suematsu H, Takata M, Yatsui K (2005) Photo and cathodoluminescence of Si/SiO2 nanoparticles produced by laser ablation. J Optoelectr Adv Mat 7:2979–2984

Grosser T, Yusuff S, Cheskis E, Pack MA, FitzGerald GA (2002) Developmental expression of functional cyclooxigenases in zebrafish. Proc Natl Acad Sci 99:8418–8423

Haberland ME, Fong D, Cheng L (1988) Malondialdehyde-altered protein occurs in atheroma of Watanabe heritable hyperlipidemic rabbits. Science 241:215–218

Habig WH, Pabst MJ, Jakoby WB (1974) Glutathione S-transferases. The first enzymatic step in mercapturic acid formation. J Biol Chem 249:7130–7139

Hazen SL, Hsu FF, Gaut JP, Crowley JR, Heinecke JW (1999) Modification of proteins and lipids by myeloperoxidase. Methods Enzymol 300:88–105

Hegazi MM, Attia ZI, Ashour OA (2010) Oxidative stress and antioxidant enzymes in liver and white muscle of Nile tilapia juveniles in chronic ammonia exposure. Aquat Toxicol 15:118–125

Jamieson T, Bakhshi R, Petrova D, Pocock R, Imani M, Seifalian AM (2007) Biological applications of quantum dots. Biomaterials 28:4717–4732

Kaisto T, Rahkila P, Marjomäki V, Parton RG, Metsikkö K (1999) Endocytosis in skeletal muscle fibers. Exp Cell Res 253:551–560

Kim JS, Yoon TJ, Yu KN, Kim BG, Park SJ, Kim HW, Lee KH, Park SB, Lee JK, Cho MH (2006) Toxicity and tissue distribution of magnetic nanoparticles in mice. Toxicol Sci 89:338–347

Kletzien RF, Harris PK, Foellmi LA (1994) Glucose-6-phosphate dehydrogenase: a "housekeeping" enzyme subject to tissue-specific regulation by hormones, nutrients and oxidant stress. FASEB J 8:174–181

Lee K-H (2007) Quantum dots for molecular imaging. J Nucl Med 48:1408–1410

Li F, Zhang Z-P, Peng J, Ciu Z-Q, Pang D-W, Li K, Wei H-P, Zhou Y-F, Wen J-K, Zhang X-E (2009) Imaging viral behavior in mammalian cells with self- assembled capsid-quantum dot hybrid particles. Small 5:718–726

Li ZH, Zlabek V, Velisek J, Grabic R, Machova J, Randak T (2010) Physiological condition status and muscle-based biomarkers in rainbow trout (Oncorhynchus mykiss), after long-term exposure to carbamazepine. J Appl Toxicol 30:197–203

Lieschke GJ, Currie PD (2007) Animal models of human disease: zebrafish swim into view. Nat Rev Genet 8:353–367

Liu T, Li L, Teng X, Huang X, Liu H, Chen D, Ren J, He J, Tang F (2011) Single and repeated dose toxicity of mesoporous hollow silica nanoparticles in intravenously exposed mice. Biomaterials 32:1657–1668

Lohr GW, Waller HD (1974) Glucose-6-phosphate dehydrogenase. In: Bergmeyer HV (ed) Methods of Enzymatic Analysis. Academic Press, New York and London, pp 744–751

Lovric J, Bazzi HS, Cuie Y, Fortin GRA, Winnik FM, Maysinger D (2005) Differences in subcellular distribution and toxicity of green and red emitting CdTe quantum dots. J Mol Med 83:377–385

Lowry OH, Rosebrough NJ, Farr AL, Randall RJ (1951) Protein measurement with the Folin-Phenol reagents. J Biol Chem 193:265–275

Mahto SK, Yoon TH, Rhee SW (2010) Cytotoxic effects of surface-modified quantum dots on neuron-like PC12 cells cultured inside microfluidic devices. Biochip J 4:82–88

Malis CD, Bonventre JV (1986) Mechanism of calcium potentiation of oxygen free radical injury to renal mitochondria: A model for post-ischemic and toxic mitochondrial damage. J Biol Chem 261:14201–14208

Månsson A, Sundberg M, Balaz M, Bunk R, Nicholls IA, Omling P, Tågerud S, Montelius L (2004) In vitro sliding of actin filaments labeled with single quantum dots. Biochem Biophys Res Commun 314:529–534

Micic OI, Sprague JR, Curtis CJ, Jones KM, Machol JL, Nozik AJ, Giessen H, Fluegel B, Mohs G, Peyghambarian N (1995) Synthesis and characterization of InP, GaP, and GaInP2 quantum dots. J Phys Chem 99:7754–7759

Mitchell DL, Fernandez AA, Nairn RS, Garcia R, Paniker L, Trono D, Thames HD, Gimenez-Conti I (2010) Ultraviolet A does not induce melanomas in a Xiphophorus hybrid fish model. Proc Natl Acad Sci 107:9329–9334

Moghimi SM, Hunter AC, Murray JC (2005) Nanomedicine: current status and future perspectives. FASEB J 19:311–330

Monteiro DA, De Almeida JA, Rantin FT, Kalinin AL (2006) Oxidative stress biomarkers in the freshwater characid fish, Brycon cephalus, exposed to organophosphorus insecticide Folisuper 600 (methyl parathion) Comparative biochemistry and physiology. Toxicology pharmacology CBP 143:141–149

Moyle PB, Cech JJJ (2004) Reproduction in fishes-an introduction in ichthyology. Prentice Hall Inc., NJ

Moylen JS, Reid MB (2007) Oxidative Stress chronic disease and muscle wasting. Muscle Nerve 35:411–429

Muller-Borer BJ, Collins MC, Gunst PR, Cascio WE, Kypson AP (2007) Quantum dot labeling of mesenchymal stem cells. J Nanobiotech 5:1–19

O'Farrell N, Houlton A, Horrocks BR (2006) Silicon nanoparticles: applications in cell biology and medicine. Int J Nanomed 1:451–472

Olaviyan CIO (1975) An introduction to West African ecology. Heinemann Educational Book Ltd, London

Paoletti F, Mocali A (1990) Determination of superoxide dismutase activity by purely chemical system based on NADP(H) oxidation. Methods Enzymol 186:209–221

Park JH, Gu L, von Maltzahn G, Ruoslahti E, Bhatia SN, Sailor MJ (2009) Biodegradable luminescent porous silicon nanoparticles for in vivo applications. Nat Mater 8:331–336

Pi QM, Zhang WJ, Zhou GD, Liu W, Cao Y (2010) Degradation or excretion of quantum dots in mouse embryonic stem cells. BMC Biotechnol 10:36–45

Powers SK, Jackson MJ (2008) Exercise -induced oxidative stress: cellular mechanisms and impact on muscle force production. Physiol Rev 88:1243–1276

Powers SK, Duarte J, Kavazis AN, Talbert EE (2010) Reactive Oxygen species are signaling molecules for skeletal muscle adaptation. Exp Physiol 95:1–9

Raisuddin S, Lee J-S (2008) Fish models in impact assessment of carcinogenic potential of environmental chemical pollutants: An appraisal of hermaphroditic Mangrove Killifish Kryptolebias marmoratus. In: Murakami Y, Nakayama K, Kitamura S-I, Iwata H, Tanabe S (eds) Interdisciplinary studies on environmental chemistry-biological responses to chemical pollutants. Terrapub, Tokyo, pp 7–15

Rajesh M, Sulochana KN, Coral K, Punitham R, Biswas J, Babu K, Ramakrishnan S (2004) Determination of carbonyl group content in plasma proteins as a useful marker to assess impairment in antioxidant defence in patients with Eales' disease. Ind J Ophtal 52:139–144

Rieger S, Kulkarmi RP, Darcy D, Fraser SE, Köster RW (2005) Quantum dots are powerful multipurpose vital labeling agents in zebrafish embryos. Dev Dyn 234:670–681

Riener C, Kada G, Gruber HJ (2002) Quick measurement of protein sulfhydryls with Ellman's reagent and with 4, 4′-dithiodipyridine. Anal Bioanal Chem 373:266–276

Rowley AF (1996) The evolution of inflammatory mediators. Mediators Inflamm 5:3–13

Rutkowska M, Strzyewski K, Iskra M, Piorunka-Stolzmann M, Majewski W (2005) Increased protein carbonyl groups in the serum of men with chronic arterial occlusion and the effect of postoperative treatment. Med Sci Monit 11:79–83

Sen CK, Packer L (1996) Antioxidant and redox regulation of gene transcription. FASEB J 10:709–720

Shacter E (2000) Quantification and significance of protein oxidation in biological samples. Drug Metab Rev 32: 307–326

Shaw BJ, Handy RD (2011) Physiological effects of nanoparticles on fish: a comparison of nanometals versus metal ions. Environ Int 37:1083–1097

Son SW, Kim JH, Kim SH, Kim H, Chung AY, Choo JB, Oh CH, Park HC (2009) Intravital imaging in zebrafish using quantum dots. Skin Res Technol 15:157–160

Sun D, Yang K, Zheng G, Li Z, Cao Y (2010) Study on effect of peptide-conjugated near-infrared fluorescent quantum dots on the clone formation, proliferation, apoptosis and tumorigenicity ability of human buccal squamous cell carcinoma cell line BcaCD885. Int J Nanomed 5:401–405

Torres-Ramos YD, Garcia-Guillen ML, Olivares-Corichi IM, Hicks JJ (2009) Correlation of Plasma Protein Carbonyls and C-reactive Protein with GOLD Stage Progression in COPD Patients. Open Resp Med J 3:61–66

Walling MA, Novak JA, Shepard JRE (2009) Quantum dots for live cell and in vivo imaging. Int J Mol Sci 10:441–491

Winterbourn CC, Metodieva D (1994) The reactions superoxide with reduced glutathione. Arch Biochem Biophys 314: 284–290

Witko-Sarsat V, Nguyen AT, Descamp S, Latsha B (1992) Microtitre plate assay for phagocyte derived taurine chloroaminea. J Clin Lab Annals 6:47–53

Witko-Sarsat V, Friedlander M, Capeillere-Blandin C, Ngnyen-Khoa T, Nguyen AT, Zingraff J, Yungers P, Deschamps-Latecha B (1996) Advanced oxidation protein products as a novel marker of oxidative stress in uremia. Kidney Int 49:1304–1313

Witko-Sarsat V, Friedlander M, Khoa TN, Capeillère-Blandin C, Nguyen AT, Cantelup S, Dayer J-M, Jungers P, Drüeke T, Descamps-Latscha B (1998) Advanced Oxidation Protein Products as Novel Mediators of Inflamation and Monocyte Activation in Chronic Renal Failure. J Immunol 161:2524–2532

Wittbrodt J, Shima A, Schartl M (2002) Medaka- a model organism from the far East. Nature Rev Genet 3:53–64

Xie G, Sun J, Zhong G, Shi L, Zhang D (2010) Biodistribution and toxicity of intravenously administered silica nanoparticles in mice. Arch Toxicol 84:183–190

Yu WW, Peng X (2002) Formation of high-quality CdS and other II-VIs semiconductor nanocrystals in noncoordinating solvents: Tunable reactivity of monomers. Angew Chemie 41:2368–2371

Zhang H, Yee D, Wang C (2008) Quantum dots for cancer diagnosis and therapy: Biological and clinical perspectives. Nanomed 3:83–91

Zhang LW, Monteiro-Riviere NA (2009) Mechanisms of quantum dot nanoparticles cellular uptake. Toxicol Sci 110:138–155

Zhu Z-J, Carboni R, Quercio JMJ, Yan B, Miranda OR, Anderton DL, Arcado KF, Rotello VM, Vachet RW (2010) Surface properties dictate uptake, distribution, excretion and toxicity of nanoparticles in fish. Small 6:2261–2265